

A Neurophysiology-Inspired Steady-State Color Appearance Model

Timo Kunkel* and Erik Reinhard†

Department of Computer Science, University of Bristol
Merchant Venturers Building, Woodland Road, Bristol BS8 1UB, UK

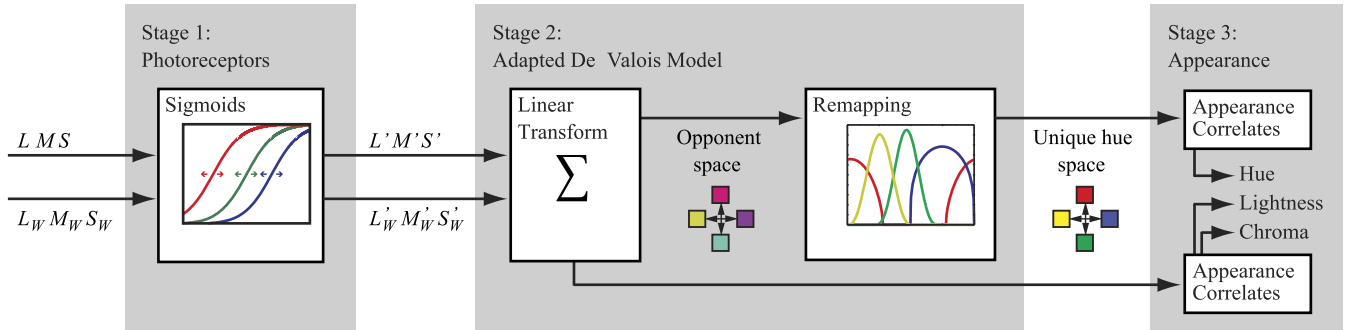


Figure 1: Stage 1 models the combined effect of both chromatic adaptation and non-linear response compression, while stage 2 offers a physiologically plausible model of perceptually unique hues. The output of the second stage is used to compute appearance correlates, which describe how a patch of colour is perceived when observed in a specific environment.

Abstract

Color appearance models predict how a patch of color is perceived under specific illumination. Here we derive a new model based on neuroscientific insights, leading to a simpler explanation of color appearance while at the same time predicting existing psychophysical data with similar accuracy for chroma, and higher accuracy for lightness and hue.

1 Introduction

The tradition in color appearance modeling is to develop improved models in a semi-incremental fashion. This has led to a family of color appearance models [Fairchild 2005], of which CIECAM02 is the most recent and currently CIE-endorsed model [CIE 2004]. Color appearance models are typically tuned to psychophysical data obtained with corresponding color or magnitude-estimation experiments [Luo and Hunt 1998], such as the LUTCHI dataset [Luo et al. 1991].

Generally, color appearance models (CAMs) consist of three steps. In the first, chromatic adaptation is modeled with a von-Kries-style transform (i.e. each color channel is treated independently [von Kries 1902]), carried out in a sharpened color space [Moroney et al. 2003]. The second step involves of non-linear response compression. Performed in a cone response space, this step models photoreceptor behaviour. The third step computes color opponent values and uses this to derive measures of lightness, hue, and chroma (as

well as others), which describe the human visual response to a colored patch in the context of an environment illuminated by a given light source.

There is at least one theoretical problem with this model. The function computed by the non-linear response compression is very close to the response compression known to occur in the photoreceptors [van Hateren 2005; van Hateren 2006]. Thus, it constitutes the first part in the chain of processing in human vision. However, in CIECAM02, it is the second step in the model. We argue that this makes the model implausible.

Further, chromatic adaptation and response compression are executed in different color spaces, presumably to fit psychophysical data. This makes that CIECAM02 cannot be viewed as a von Kries model: the three channels are not treated independently. As the human cones are assumed to operate independently of one another, it is undesirable to introduce channel interdependencies at this stage of the model.

We argue that both problems can be solved by combining the chromatic adaptation and response compression, leading to a single set of equations that can be thought of as modeling the cone response.

After the response compression step, CIECAM02 continues with the computation of hue angle, followed by further color correlates such as hue, lightness and chroma. The hue is an adjustment of the hue angle to match psychophysical data. We also note that hue itself is used in the computation of chroma. Neither of these features are likely to model human vision, which we argue on the basis of communication bottlenecks.

In the path between the retina and the brain, only one transmission bottleneck exists, which is the optic nerve. The color opponent space used by the ganglion cells (whose axons form the optic nerve) is to some extent decorrelated [Ruderman and Bialek 1994; Ruderman et al. 1998] thereby maximizing the information transfer within the available bandwidth. However, downstream in the brain no such bottlenecks are encountered. Instead, the information stream proliferates and merges with feedback paths from elsewhere in the brain.

*e-mail: kunkel@cs.bris.ac.uk

†e-mail: reinhard@cs.bris.ac.uk

The computation of hue, on the other hand, is an aggregation of color opponent information into a single number. It carries less information than the color opponent values from which it was derived. It is therefore unlikely that even if hue is encoded explicitly in the brain, that it is subsequently used to compute chroma. We would therefore favor a model in which hue is computed as a final color appearance correlate, rather than an intermediary step used to compute others. This is modeled explicitly in our approach, as discussed next.

2 Motivation and Overview

There are two components to our new algorithm that are motivated and described in this section. Section 3 then presents the detailed equations, allowing the model to be implemented and reproduced. The two innovations presented in this paper are a new transform which combines chromatic adaptation with the non-linear response compression. We show that this formulation is simpler, and therefore theoretically more plausible, while at the same time providing the same accuracy that CIECAM02 delivers using separate color spaces. The second improvement is achieved by better modeling the opponent spaces which ultimately lead to the computation of the perceptually unique hues. The resulting model has a higher accuracy, has a solid foundation in results obtained from neurophysiology, while still being computationally efficient. Moreover, the model is invertible, so that it can be used in imaging applications.

2.1 Combined Chromatic Adaptation and Non-Linear Compression

Although chromatic adaptation and response compression treat each of the three color channels independently, the use of separate color spaces means that the full model is no longer compatible with the von Kries hypothesis (independent adaptation of each photoreceptor) [von Kries 1902]. More importantly, even if photoreceptors would receive lateral feedback from half cells, this would not lead to the internal computation of a sharpened color space. We therefore argue that by placing the chromatic adaptation before the non-linear response compression, CAMs deviate from physiological evidence by suggesting that cones adapt in a sharpened color space before applying the response compression.

Instead, we show that chromatic adaptation can be modeled using the adaptation mechanism afforded by the non-linear response compression alone, leading to the control flow outlined in Figure 1. With this approach, the model once more adheres to the von Kries hypothesis [von Kries 1902], which thereby after more than 100 years continues to be the simplest model that explains all relevant appearance phenomena. Furthermore, it obviates the need for a separate chromatic adaptation step.

Photoreceptor responses are well modeled by sigmoidal compression functions, such as the Naka-Rushton equation [Naka and Rushton 1966] which is given by $V = L^n / (L^n + \sigma^n)$, where n is a positive constant, usually smaller than 1, which determines the steepness of the function. The response V is related to the incident luminance L by means of the semi-saturation constant σ , which can be varied to model adaptive processes [Dowling 1987]. In color appearance models this equation is normally executed in the SML cone response space on each of the color channels independently, albeit with a shared semi-saturation constant. This suggests that all cone types are adapted to the environment identically; hence the need for a separate chromatic adaptation transform.

The crucial innovation presented here is that we make the semi-saturation constant dependent on the illuminant, in a manner consistent with existing psychophysical appearance data. The new model

for the S channel is given by $V_S = S^n / (S^n + f(S_W)^n)$. The M and L channels are computed similarly. The semi-saturation constant is computed with a simple function f , given by $f(S_W) = (DS_W + (1-D))^n$, and takes into account both the illuminant $S_W M_W L_W$ and the degree of adaptation D . The latter is important to distinguish between reflective and self-luminous surfaces, which cause the human visual system to adapt differently. The resulting formulation provides a channel-independent model for the steady-state behavior of photoreceptors, while at the same time accounting for chromatic adaptation.

2.2 Appearance Correlates

A second innovation presented here relates to the choice of color opponent processing, which is a required intermediate step for the prediction of hue. In the human visual system, the photo-receptor output is eventually encoded into a decorrelated color opponent space which the retinal ganglion cells transmit to the lateral geniculate nucleus (LGN) [Guth et al. 1969]. The chromatic axes in this opponent space are often labeled 'red - green' and 'yellow - blue'. However, the actual orientations of these axes are closer to 'pinkish-red - cyan' and 'greenish-yellow - violet' [Derrington et al. 1984]. They therefore do not coincide with the perceptually unique hues red, green, yellow, and blue which are required for appearance modeling. It can be argued that these perceptual colors are generated from the ganglion opponent space later on in the visual pathway [De Valois and De Valois 1993].

In CAMs this is modeled by a hue correction step motivated by the need to fit psychophysical data. As this approach does not offer a good explanation of hue perception, we propose to incorporate a neurophysiological model of color perception instead (see Figure 1). In particular, De Valois and colleagues have argued in favor of a three-stage color model, which explicitly models the difference between standard color opponency and the color space spanned by the perceptually unique hues [De Valois and De Valois 1996]. As this approach assumes adaptation to an equal-energy illuminant, we modify this model to take as input the signal produced by our combined chromatic adaptation and non-linear response compression stage.

In their model, they recombine an SML signal by a linear combination to form a decorrelated opponent system, also taking into account the relative number of cones for each type (S:M:L = 1:5:10). The geniculate opponent system is then linearly recombined to form a 2-dimensional space (a, b) with the axes approximately corresponding to the four unique hues.

As shown by De Valois et al. [2000], this opponent space is not yet linear, although an approximate hue can be computed with $h = \tan^{-1}(b/a)$. To produce a more accurate hue descriptor, they found that the axes require a further small reorientation, as well as sharpening. This can be achieved by passing the hue value h through an exponentiated sinusoid, creating four new axes $a_i = k_i \cos^{m_i}(s_i - h)$, with $i \in [1, 4]$. The amount of sharpening is given by the positive exponent m_i , whereas the values s_i specify the new orientations, and k_i give the relative amplitudes. In this space, hue is then computed using $h' = \tan^{-1}((a_4 - a_2)/(a_3 - a_1))$. This procedure sharpens the signal, and creates hues that correspond well with psychophysical measurements, as shown below.

We fit the hue descriptor to the LUTCHI dataset [Luo 1997], which consists of 8 groups and 48 usable phases representing various viewing conditions. Each group contains colorimetric data that can be used as input to our model, as well as appearance correlates for lightness, hue, and chroma to compare our output against. The data was fit by means of unconstrained non-linear optimization (the

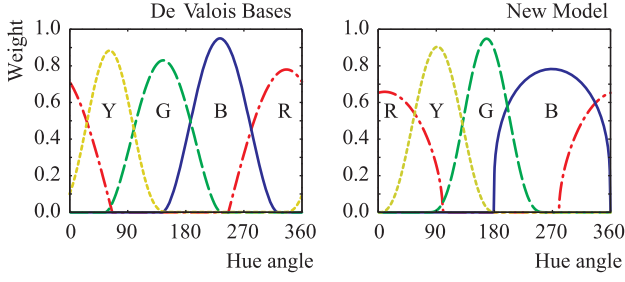


Figure 2: The basis functions experimentally derived by De Valois and the ones obtained by optimizing these to the LUTCHI dataset.

Nelder-Mead simplex method), allowing us to determine amplitude k_i , offset s_i , and exponent m_i for the sinusoidal sharpening.

Figure 2 shows the hue basis functions experimentally derived by De Valois [1997] and the ones obtained by our optimization. It is interesting to note that although we optimized our hue basis functions against a different psychophysical dataset, we find that they still match reasonably well to De Valois' experimentally determined functions [De Valois et al. 1997]. Thus, we conclude that the color model proposed by De Valois is supported by the LUTCHI dataset.

The importance of this finding is that although their three-stage model was developed for color out of context, the model is also applicable to colors perceived in a specific context. Thus, we show for the first time that De Valois' model is suitable for color appearance modeling.

This leaves us with the computation of lightness and chroma to arrive at a more complete description of color perception. The geniculate opponent system as well as the compressed response signal can also be used to compute these appearance correlates. In particular, we have found that contrary to current practise, chroma does not require the computation of a hue descriptor. By computing these correlates directly from low level signals, we are able to optimize these correlates against the same psychophysical dataset. This yields results that are similar for chroma, while for most test conditions we achieve more accurate results for lightness and hue than the current state-of-the-art.

3 Forward Algorithm

Here we present the equations to our neurophysiological model. The input values are the XYZ values of the stimulus, the adapting white $X_W Y_W Z_W$, the luminance of the adapting field L_A in cd/m^2 , the relative luminance factor of the background Y_b , and the surround (usually either *average*, *dim* or *dark*).

3.1 Preliminary Computations

To ensure our model is compatible with common conventions in color appearance modeling, we rely on several preliminary computations that are retained from the CIECAM02 model.

Dependent on which surround condition is selected (*average*, *dim*, or *dark*), the corresponding values for F , c , and N_c can be determined using Table 1. We can then compute F_L :

$$k = 1/(5L_A + 1) \quad (1)$$

$$F_L = 0.2k^4(5L_A) + 0.1(1 - k^4)^2(5L_A)^{1/3} \quad (2)$$

Then, the following intermediate parameters are computed:

Table 1: Viewing condition parameters for different surrounds

Surround	F	c	N_c
Average	1.0	0.69	1.0
Dim	0.9	0.59	0.95
Dark	0.8	0.525	0.8

$$n = \frac{Y_b}{Y_W} \quad (3)$$

$$N_{bb} = N_{cb} = 0.725 \left(\frac{1}{n} \right)^{0.2} \quad (4)$$

$$z = 1.48 + \sqrt{n} \quad (5)$$

The value n is a function of the luminance factor of the background which can then be used to calculate N_{bb} , N_{cb} and z which will be used later in the computation of the appearance correlates.

Furthermore, the luminance of the adopted whitepoint can influence the degree D to which an observer adapts to that white point. The degree of adaptation D is a function of both the surround and L_A and could in theory range from 0 for no adaptation to the adopted white point up to 1 for full adaptation. In practise, D will not be below 0.65 for a dark surround and will exponentially converge to 1 for average surrounds. The degree of adaptation is given by:

$$D = F - \left(\frac{F}{3.6} \right) \exp \left(\frac{-L_A - 42}{92} \right) \quad (6)$$

3.2 Chromatic Adaptation and Non-Linear Response Compression

The first part of our model consists of the non-linear response compression, which incorporates chromatic adaptation by means of an appropriate manipulation of the semi-saturation constant. Given that this stage models photoreceptor behavior, we first transform the tristimulus values for the stimulus (X, Y, Z) as well as the whitepoint (X_w, Y_w, Z_w) to SML cones space, using the Hunt-Pointer-Estevéz transform:

$$\begin{bmatrix} L \\ M \\ S \end{bmatrix} = \begin{bmatrix} 0.3897 & 0.6890 & -0.0787 \\ -0.2298 & 1.1834 & 0.0464 \\ 0.0000 & 0.0000 & 1.0000 \end{bmatrix} \begin{bmatrix} X \\ Y \\ Z \end{bmatrix} \quad (7)$$

The semi-saturation constant σ is then computed with:

$$\sigma_L = 27.13^{1/0.42} (D(L_W/100) + (1 - D)) \quad (8a)$$

$$\sigma_M = 27.13^{1/0.42} (D(M_W/100) + (1 - D)) \quad (8b)$$

$$\sigma_S = 27.13^{1/0.42} (D(S_W/100) + (1 - D)) \quad (8c)$$

where $(L_W, M_W, S_W)^T$ is the tristimulus value of the white point and D is the degree of adaptation. The non-linear response compression is then given by:

$$L' = 400 \frac{(F_L L/100)^{0.42}}{(F_L L/100)^{0.42} + \sigma_L^{0.42}} + 0.1 \quad (9a)$$

$$M' = 400 \frac{(F_L M/100)^{0.42}}{(F_L M/100)^{0.42} + \sigma_M^{0.42}} + 0.1 \quad (9b)$$

$$S' = 400 \frac{(F_L S/100)^{0.42}}{(F_L S/100)^{0.42} + \sigma_S^{0.42}} + 0.1 \quad (9c)$$

These calculations are carried out for both the stimulus and the white point, resulting in $(L', M', S')^T$ and $(L'_W, M'_W, S'_W)^T$ respectively. These values are intermediary, and form the input to the second step of our model.

3.3 Computation of Appearance Correlates

On the basis of the non-linearly compressed values computed in the preceding section, as well as the preliminary values computed in Section 3.1, we can now compute the appearance correlates hue, chroma, and lightness.

The weights in the following equations are optimized against the LUTCHI dataset which resulted in separate calculations for lightness, chroma and hue. We excluded the neutral values, as these are not valid to derive color appearance models. To be consistent in modeling cone photoreceptor behavior for related colors we furthermore excluded the LUTCHI sets R-VL 7 to 12 as they are representing brightness and colorfulness values instead of lightness and chroma. Also, the BIT subset was excluded (BIT 1 to 5) as it was compiled to investigate color appearance under mesopic conditions (stimuli under low luminance levels where both rods and cones are excited).

To compute the appearance correlate for lightness, we first need to compute the achromatic response both for the patch and the illuminant:

$$A = N_{bb} (4.19L' + M' + 1.17S') \quad (10)$$

$$A_W = N_{bb} (4.19L'_W + M'_W + 1.17S'_W) \quad (11)$$

The weights applied to L' , M' , and S' stem from our optimization. Lightness J is then computed with the following equation:

$$J = 106.5 (A/A_W)^{cz} \quad (12)$$

The computation of chroma relies on a normalization constant d as well as a color opponent space which is represented by a_c and b_c :

$$\begin{bmatrix} a_c \\ b_c \\ d \end{bmatrix} = \begin{bmatrix} -4.5132 & 3.9899 & 0.5233 \\ -4.1562 & 5.2238 & -1.0677 \\ 7.3984 & -2.3007 & -0.4156 \end{bmatrix} \begin{bmatrix} L' \\ M' \\ S' \end{bmatrix} \quad (13)$$

These values are then inserted into intermediary value t together with the induction factors N_c and N_{cb} :

$$t = \frac{(N_c N_{cb} \sqrt{a_c^2 + b_c^2})}{d} \quad (14)$$

Note in particular, that the hue angle is no longer used in the computation of chroma:

$$C = (10^3 t)^{0.9} \sqrt{\frac{J}{100} (1.64 - 0.29^n)^{0.73}} \quad (15)$$

For the computation of hue, first a color opponent space with a and b axes is computed. Note that this is a different opponent space than the one used for chroma:

$$\begin{bmatrix} a_h \\ b_h \end{bmatrix} = \begin{bmatrix} -15.4141 & 17.1339 & -1.7198 \\ -1.6010 & -0.7467 & 2.3476 \end{bmatrix} \begin{bmatrix} L' \\ M' \\ S' \end{bmatrix} \quad (16)$$

followed by the computation of an intermediate hue:

$$h = \tan^{-1} \left(\frac{b_h}{a_h} \right) \quad (17)$$

Following models from neurophysiology, we can now model the conversion from the ganglion-derived decorrelated color space to perceptually unique hues using a non-linear transform. Once more through optimizing the coefficients, we obtained the following transform:

$$r_p = \max \left(0, 0.6581 \cos^{0.5390} (9.1 - h) \right) \quad (18)$$

$$g_p = \max \left(0, 0.9482 \cos^{2.9435} (167.0 - h) \right) \quad (19)$$

$$y_p = \max \left(0, 0.9041 \cos^{2.5251} (90.9 - h) \right) \quad (20)$$

$$b_p = \max \left(0, 0.7832 \cos^{0.2886} (268.4 - h) \right) \quad (21)$$

The values r_p , g_p , y_p , and b_p are plotted against h in Figure 2 where they are also compared against the basis functions proposed by De Valois et al. [1997]. The differences are due to the optimization against LUTCHI. Note that we seeded the optimization process with the De Valois bases. The resulting values can now be mapped into a perceptual color opponent space, forming red-green and yellow-blue opponent pairs:

$$a'' = r_p - g_p \quad (22)$$

$$b'' = y_p - b_p \quad (23)$$

followed by the usual hue computation:

$$h' = \tan^{-1} \left(\frac{b''}{a''} \right) \quad (24)$$

4 Inverse Model

In imaging applications, color appearance models can be used to take an image intended for a specific viewing environment, and prepare it for a different viewing environment. To achieve this, the model is run in forward mode using the parameters associated with the initial viewing environment. The resulting appearance correlates are then used as input to the inverse model, with substitution of parameters describing the second viewing environment. In the following, we use the subscript d to indicate the second (destination or display) environment.

To compute the inverse model, we begin by repeating all the calculations outlined in Section 3.1, but using the inputs associated with the second environment. We also compute $(L'_{W,d}, M'_{W,d}, S'_{W,d})$ from $(X_{W,d}, Y_{W,d}, Z_{W,d})$ and from those values $A_{W,d}$. Lastly, we compute the semi-saturation constants in forward mode, yielding $(\sigma_{L,d}, \sigma_{M,d}, \sigma_{S,d})$.

The model inversion then begins with values for J , C and the (a_c, b_c) opponent pair. Note that the computation of hue from (L', M', S') does not involve any other variables, which means that we do not need to invert this part of the model. We therefore proceed by computing intermediary parameter t_d as follows:

$$t_d = 10^{-3} \left(\frac{C}{\sqrt{J/100} (1.64 - 0.29^{n_d})^{0.73}} \right)^{1/0.9} \quad (25)$$

Using t from the forward transform, we now scale both a_c and b_c by their ratio:

$$a'_c = a_c \frac{t_d}{t} \quad (26a)$$

$$b'_c = b_c \frac{t_d}{t} \quad (26b)$$

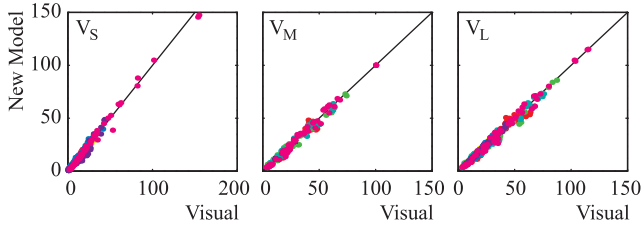


Figure 3: The V_S , V_M , and V_L outputs of our model (Stage 1) plotted against the results of the corresponding color datasets.

We then compute a new value for the achromatic signal A_d :

$$A_d = A_{W,d} \left(\frac{J}{106.5} \right)^{1/c_{azd}} \quad (27)$$

We now have A_d , a'_c , and b'_c , of which we can compute L'_d , M'_d , and S'_d :

$$\begin{bmatrix} L'_d \\ M'_d \\ S'_d \end{bmatrix} = \begin{bmatrix} -4.5132 & 3.9899 & 0.5233 \\ -4.1562 & 5.2238 & -1.0677 \\ 4.19 & 1.00 & 1.17 \end{bmatrix}^{-1} \begin{bmatrix} a'_c \\ b'_c \\ A_d/N_{bb,d} \end{bmatrix}, \quad (28)$$

where we have taken coefficients from Equations 10 and 13. The final step is to compute the inverse of the sigmoidal response compression step:

$$L_d = \frac{100}{F_{L,d}} \left(\frac{\sigma_{L_d} (L'_d - 0.1)}{400 - (L'_d - 0.1)} \right)^{1/0.42} \quad (29a)$$

$$M_d = \frac{100}{F_{L,d}} \left(\frac{\sigma_{M_d} (M'_d - 0.1)}{400 - (M'_d - 0.1)} \right)^{1/0.42} \quad (29b)$$

$$S_d = \frac{100}{F_{L,d}} \left(\frac{\sigma_{S_d} (S'_d - 0.1)}{400 - (S'_d - 0.1)} \right)^{1/0.42} \quad (29c)$$

The values (L_d, M_d, S_d) can then be converted to XYZ , and from there to a device-dependent color space for final display.

5 Results

The model presented in this paper consists of two innovations, which are evaluated separately. The chromatic adaptation and non-linear response compression are compared against existing corresponding color datasets, whereas the final output of our algorithm is compared against CIECAM02. Both the intermediary stage and the final output are compared against the LUTCHI dataset.

To assess the predictive power of the combined chromatic adaptation and non-linear response compression, we have compared it against corresponding color datasets which form the basis for other chromatic adaptation transforms [Li et al. 2002]. Specifically we have compared against the CSAJ [Mori et al. 1991], Kuo and Luo [1995], Lam and Rigg [1985], Helson et al. [1952], Breneman [1987], and the Braun and Fairchild [1996] datasets. We also compare this intermediate step against CIECAM02 [Moroney et al. 2003].

Figure 3 shows the V_S , V_M , and V_L outputs of our model plotted against the results of the corresponding color datasets. The RMS error based on 586 stimuli out of 7 different corresponding datasets is 28.31 for our model, 28.40 for CIECAM02 and 28.57 for the task carried out by human observers. The results show that our

new model performs as well as CIECAM02 in predicting the corresponding color datasets, while offering a simpler physiological explanation of chromatic adaptation.

To determine the validity of the full color appearance model we evaluate its predictive power by comparing the output of both CIECAM02 and our model against the LUTCHI dataset. To avoid over-fitting, we have repeatedly and randomly split the data into training and test sets. The training set is then used for optimization, whereas the test set is used for evaluation. This ensures that the results will generalize, and are not dependent on particularities that might be inadvertently encoded in each of the groups.

The resulting mean RMS error of our model with respect to the LUTCHI psychophysical data (standard deviations in brackets) over 34 optimization runs is 7.97 (0.40) for lightness, 8.68 (0.65) for chroma, and 12.40 (0.27) for hue. The corresponding values computed for CIECAM02 performance are 9.22, 9.04 and 21.70 respectively. These results show that the accuracy of lightness, and in particular hue, has improved. Moreover, Figure 4 demonstrates that the reduced RMS error is achieved by improving across all groups and phases, meaning that our algorithm predicts appearance data better over a wide variety of viewing conditions.

6 Conclusions

In summary, we have shown that a model of color appearance can be constructed by combining chromatic adaptation with non-linear response compression. This results in a straightforward steady-state von Kries-type model [von Kries 1902] which is consistent with current knowledge of photoreceptor behavior, and exhibits sufficient expressiveness to provide the basis of a color appearance model which performs at least as well as CIECAM02.

A second observation explored here is that the orientation of color opponent axes is close to, but different from the orientation of the perceptually unique hues of red, green, yellow, and blue. Rather than applying an ad-hoc correction, we have shown that De Valois' three-stage color model [1996] is compatible with color appearance data. A straightforward optimization of its parameters allows the computation of hues that are closely matched to psychophysical color appearance data. This constitutes a departure from the norm in color appearance modeling which tends to rely on hue predictors based on ganglion-type opponency. Overall, our color appearance model integrates insights from color- and neuroscience, while at the same time leading to improved color appearance predictions.

Acknowledgments

We are grateful to Dolby Canada for their financial support. We would also like to thank Gerwin Damberg, Peter Longhurst, Helge Seetzen, Greg Ward, Tania Pouli and Ben Long for helpful discussions and comments.

References

- BRAUN, K., AND FAIRCHILD, M. 1996. Psychophysical generation of matching images for cross-media color reproduction. In *Proceedings of the 4th Color Imaging Conference*, 214–220.
- BRENEMAN, E. J. 1987. Corresponding chromaticities for different states of adaptation to complex visual fields. *Journal of the Optical Society of America A* 4, 1115–1129.
- CIE. 2004. CIE TC8-01 technical report. a colour appearance model for color management systems: CIECAM02. Tech. rep., CIE.

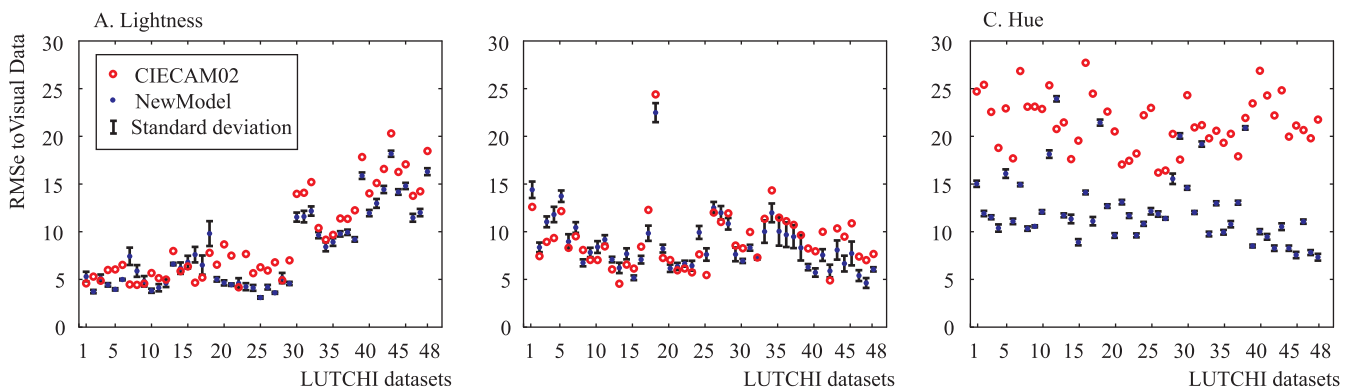


Figure 4: The RMS error for both our new model and CIECAM02 compared to the 48 relevant LUTCHI datasets. The error bars reflect the spread over the different optimisation runs.

- DE VALOIS, R., AND DE VALOIS, K. K. 1993. A multi-stage color model. *Vision Research* 33, 8, 1053–1065.
- DE VALOIS, R. L., AND DE VALOIS, K. K. 1996. On “a three-stage color model”. *Vision Research* 36, 6, 833–836.
- DE VALOIS, R. L., DE VALOIS, K. K., SWITKES, E., AND MAHON, L. 1997. Hue scaling of isoluminant and cone-specific lights. *Vision Research* 37, 7, 885–897.
- DE VALOIS, R. L., COTTARIS, N. P., EL FAR, S. D., MAHON, L. E., AND WILSON, J. A. 2000. Some transformations of color information from lateral geniculate nucleus to striate cortex. *Proceedings of the National Academy of Sciences of the United States of America* 97, 9, 4997–5002.
- DERRINGTON, A. M., KRAUSKOPF, J., AND LENNIE, P. 1984. Chromatic mechanisms in lateral geniculate nucleus of macaque. *Journal of Physiology* 357, 1, 241–265.
- DOWLING, J. E. 1987. *The retina: an approachable part of the brain*. Belknap Press of Harvard University Press, Cambridge, Mass. (USA).
- FAIRCHILD, M. D. 2005. *Color Appearance Models*, 2nd ed. Wiley-IS&T Series in Imaging Science and Technology.
- GUTH, S., DONELY, N., AND MARROCCO, R. 1969. On luminance additivity and related topics. *Vision Research* 9, 537–575.
- HELSON, H., JUDD, D., AND WARREN, M. 1952. Object-color changes from daylight in incandescent filament illumination. *Illumination Engineering* 47, 221–233.
- KUO, W., LUO, M., AND BEZ, H. 1995. Various chromatic adaptation transforms tested using new colour appearance data in textiles. *Colour Research and Application* 20, 313–327.
- LAM, K. 1985. *Metamerism and Colour Constancy*. PhD thesis, University of Bradford.
- LI, C., LUO, M. R., RIGG, B., AND HUNT, R. W. G. 2002. CMC 2000 chromatic adaptation transform: CMCCAT2000. *Color Research & Application* 27, 1, 49–58.
- LUO, M. R., AND HUNT, R. W. G. 1998. Testing colour appearance models using corresponding-colour and magnitude-estimation data sets. *Color Research & Application* 23, 3, 147–153.
- LUO, M. R., CLARKE, A., RHODES, P., SCHAPPO, A., SCRIVNER, S., AND TAIT, C. 1991. Quantifying colour appearance. Part I LUTCHI colour appearance data. *Color Research and Application* 16, 166–180.
- LUO, M. R. 1997. Communications and comments: Using the LUTCHI colour appearance data. *Color Research and Application* 20, 414–417.
- MORI, L., SOBAGAKI, H., KOMATSUBARA, H., AND IKEDA, K. 1991. Field trials on CIE chromatic adaptation formula. *Proceedings of the CIE 22nd Session*, 55–58.
- MORONEY, N., FAIRCHILD, M., R.W.G.HUNT, LI, C., LUO, M. R., AND NEWMAN, T. 2003. The CIECAM02 color appearance model. *IS&T/SID Tenth Color Imaging Conference*, 23–27.
- NAKA, K. I., AND RUSHTON, W. A. H. 1966. S-potentials from luminosity units in the retina of fish (Cyprinidae). *Journal of Physiology* 185, 587–599.
- RUDERMAN, D., AND BIALEK, W. 1994. Statistics of natural images: Scaling in the woods. *Physical Review Letters* 73, 814–817.
- RUDERMAN, D., CRONIN, T., AND CHIAO, C. 1998. Statistics of cone responses to natural images: implications for visual coding. *Journal of the Optical Society of America A* 15, 2036–2045.
- VAN HATEREN, H. 2005. A cellular and molecular model of response kinetics and adaptation in primate cones and horizontal cells. *Journal of Vision* 5, 4, 331–347.
- VAN HATEREN, H. 2006. Encoding of high dynamic range video with a model of human cones. *ACM Transactions on Graphics* 25, 4, 1380–1399.
- VON KRIES, J. 1902. Chromatic adaptation. *Festschrift der Albert-Ludwigs-Universität Freiburg* 145. English translation in *Sources of Color Vision*, D. L. MacAdam, ed., (MIT, 1970), pp. 109–119.